Measurement and Model Identification of Semiconductor Devices

JOSEF DOBEŠ MARTIN GRÁBNER
Department of Radio Engineering, Faculty of Electrical Engineering
Czech Technical University in Prague
Technická 2, 16627 Praha 6
Czech Republic

dobes@fel.cvut.cz http://www.cvut.cz

Abstract: Current models of semiconductor devices are very sophisticated, especially ones for BJT and MOSFET. The equations of such models contain typically one hundred parameters. Therefore, a measurement and particularly identification of full set of parameters is very difficult. In the paper, an optimization method is presented which is usable for identifications of even very complicated models with a relatively small number of iterations. The algorithm has been implemented into the original software tool called C.I.A. (Circuit Interactive Analyzer) into its static and dynamic analysis modes. Hence, the identification is able to identify both DC and capacitance models of semiconductor devices. The process is demonstrated in the paper using various transistors.

Key-Words: Modeling, semiconductor device, measurement, parameter extraction, optimization, BJT, MOSFET

1 Introduction

The C.I.A. optimization algorithm seeks to find up to 25 (in the current stable version of the program) unknown parameters of the circuit for fulfillment of user-specified requirements. The algorithm starts the analyses sequentially and changes these parameters after each of them to gradually fulfill the user's requirements.

2 The C. I. A. Optimization Algorithm

Let us assume that some two circuit outputs are to be monitored in three points as seen in Fig. 1. The circles mark user-specified requirements for the outputs and the squares mark values of the outputs obtained after an analysis. The algorithm seeks to minimize the sum of squares of differences between them

$$S\left(x_1,\ldots,x_n\right)=\sum_{k=1}^{m}R_k^2\left(x_1,\ldots,x_n\right),\ n\leqq m, \quad (1)$$

where the unknown optimized parameters of a circuit are marked by $x_1,\ldots,x_n$, and $R_k,\ k=1,\ldots,m$ are the differences.

An extreme of the function of n variables (1) can be found in the standard way, i. e.

$$\nabla S=\sum_{k=1}^{m}2R_k\nabla R_k=\mathbf{0}. \quad (2)$$

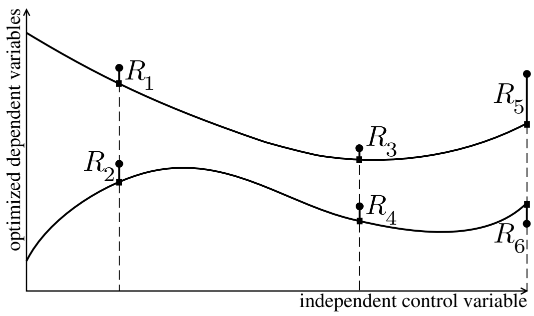

Figure 1: A diagram of a typical optimization task.

After a standard derivation [1], the generalized least-squares procedure is obtained applying the condition (2)

$$\mathbf{J}^{\mathrm{t}}\mathbf{J}\,\Delta\mathbf{x}^{(l)}=-\mathbf{J}^{\mathrm{t}}\,\mathbf{r},\ \mathbf{x}^{(l+1)}=\mathbf{x}^{(l)}+\Delta\mathbf{x}^{(l)},$$
$$l=1,\ldots,l_{\max}, \quad (3)$$

where l is the iteration index and

$$r_k=R_k\left[\mathbf{x}^{(l)}\right],\ \frac{\partial r_k}{\partial x_i}=\frac{\partial R_k}{\partial x_i}\left[\mathbf{x}^{(l)}\right],$$
$$\mathbf{J}=\left[\begin{array}{ccc}\dfrac{\partial r_1}{\partial x_1} & \cdots & \dfrac{\partial r_1}{\partial x_n}\\ \vdots & & \vdots\\ \dfrac{\partial r_m}{\partial x_1} & \cdots & \dfrac{\partial r_m}{\partial x_n}\end{array}\right],$$
$$k=1,\ldots m,\ i=1,\ldots,n.$$

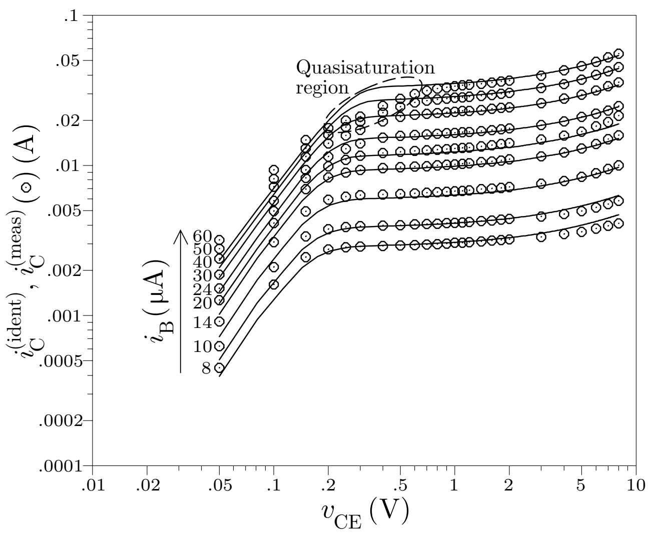

Figure 2: Forward DC characteristics of BJT KC508.

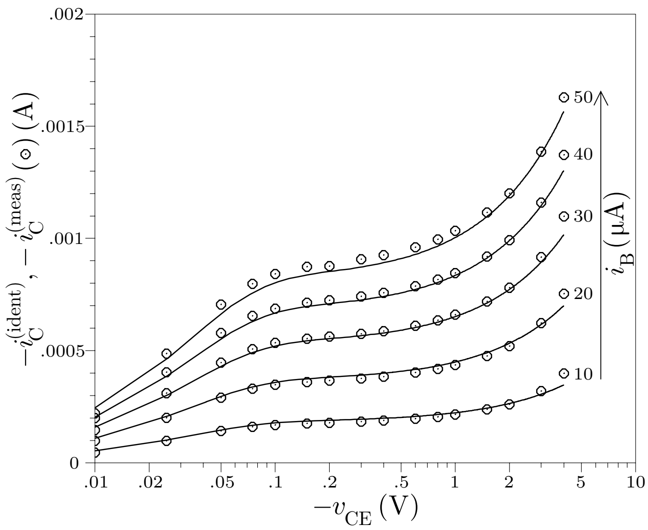

Figure 3: Reverse DC characteristics of BJT KC508.

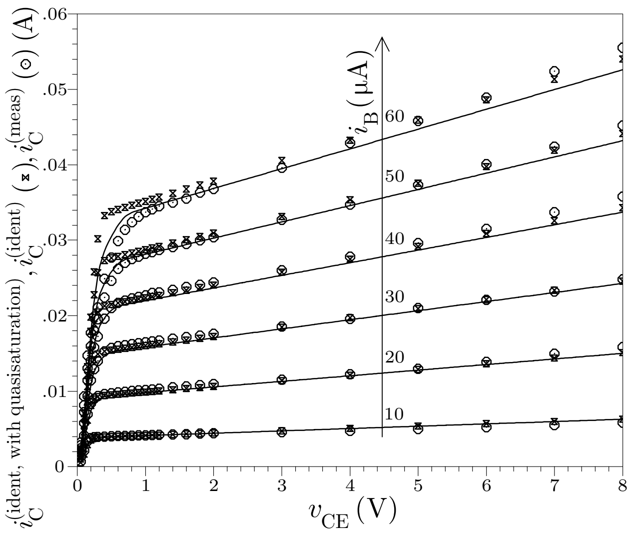

Figure 4: Impact of quasisaturation model for BJT identification.

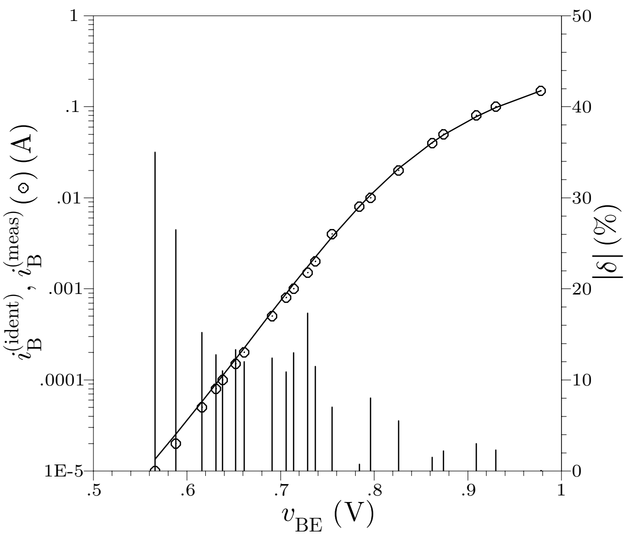

Figure 5: Input characteristic of KC508 (collector disconnected).

The generalized least-squares procedure is very fast, but sometimes insufficiently stable. For this reason, the method is combined with the gradient one

$$\Delta\mathbf{x}^{(l)} = -2\,\mathbf{J}^{\mathrm{t}}\mathbf{r},\; l = 1, \ldots, l_{\max}$$

to the reliable Levenberg-Marquardt modification of (3)

$$\left[\mathbf{J}^{\mathrm{t}}\mathbf{J} + \lambda^{(l)}\mathbf{1}\right]\Delta\mathbf{x}^{(l)} = -\mathbf{J}^{\mathrm{t}}\mathbf{r},\; \mathbf{x}^{(l+1)} = \mathbf{x}^{(l)} + \Delta\mathbf{x}^{(l)},\quad l = 1, \ldots, l_{\max}, \tag{4}$$

where $\mathbf{1}$ is unit matrix and $\lambda^{(l)}$ is a scalar iteration-dependent factor. There are many ways to optimally determine that factor for each iteration – the most sophisticated ones use an estimation based on eigenvalues of the Jacobian in (4) [2]. However, simpler empirical ways are mostly also successful [1]. The C.I.A. program also contains a version of the empirical methods (however, a way based on the eigenvalues is also possible) which seeks to minimize the $\lambda^{(l)}$ factor sequentially (i. e., to make the generalized least-squares method more influential at the end of the process, which is natural):

$$\lambda^{(1)} = 1,\qquad \lambda^{(l+1)} = \frac{\lambda^{(l)}}{5}. \tag{5}$$

However, this monotone decay must be interrupted (and therefore the gradient method must be sometimes made

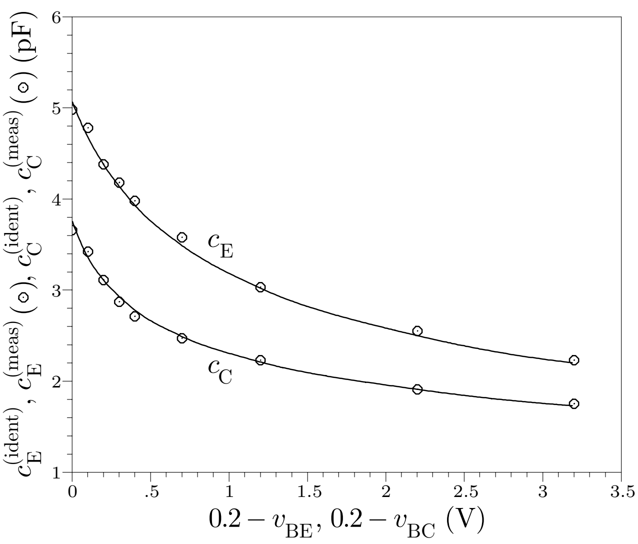

Figure 6: Collector and emitter junction capacitances of KC508.

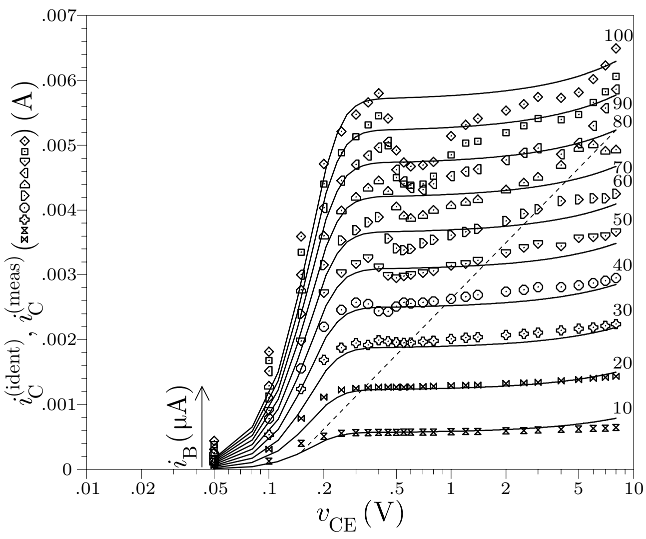

Figure 8: Forward DC characteristics of microwave BJT KT391.

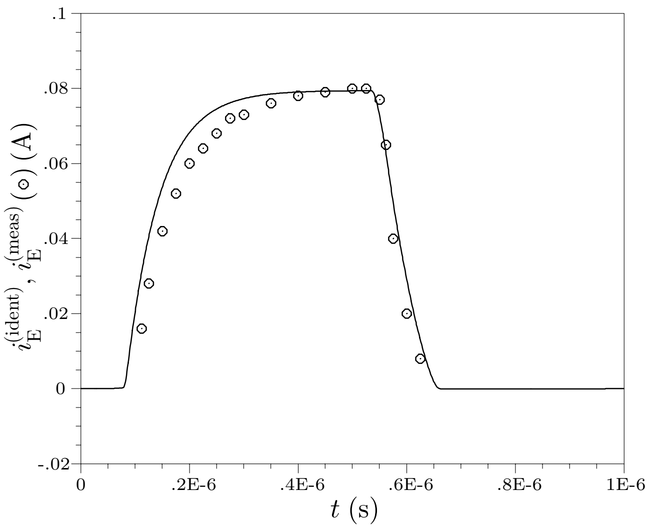

Figure 7: Identification of transit time model parameters of KC508.

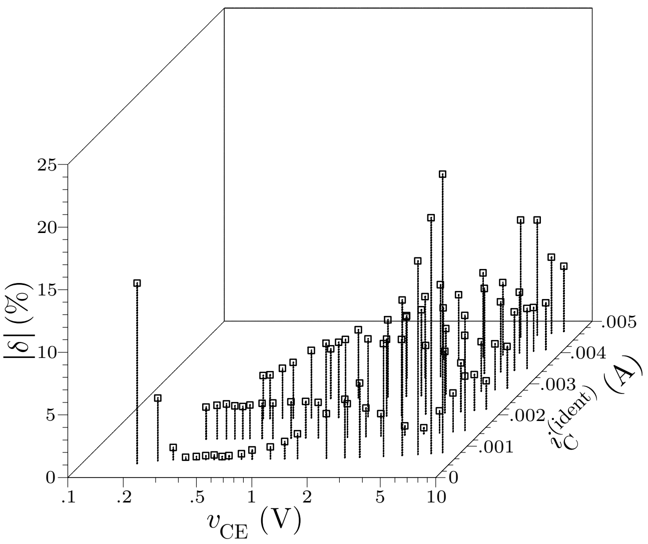

Figure 9: Relative identification errors in the selected stable area.

more influential) when the method seems to diverge:

$$\text{if } \; l > 1 \;\wedge\; S^{(l)} \geqq \min_{j=1}^{l-1} S^{(j)} \; \text{ then}$$
$$\mathbf{x}^{(l)} := \mathbf{x}^{(l-1)},\; \lambda^{(l)} := \lambda^{(l)} 5^2,$$

where the first multiplication by 5 compensates the division by 5 in (5) and the second multiplication by 5 increases that scalar factor.

Unfortunately, the method described above is insufficient for the majority class of the circuit optimization problems. Thus, an improved method has been implemented to the CIA program.

The improvement consists in the following steps:

- The differences defined in (3) *must* be normalized;
- These differences should also be weighted;
- The Jacobian **J** in (4) *must* be normalized too;
- The Jacobian can quickly be evaluated by sensitivities;
- Evaluating the Jacobian is not necessary in each iteration;
- Possible divergence of iterations (4) can be damped.

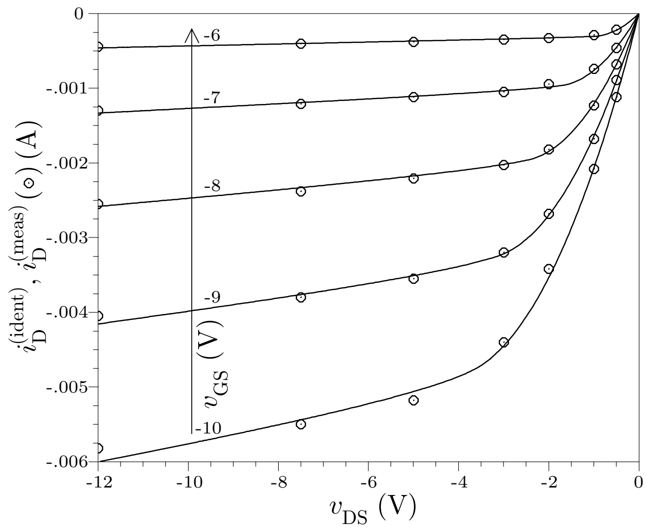

Figure 10: Forward DC characteristics of enh PMOSFET 2N3608.

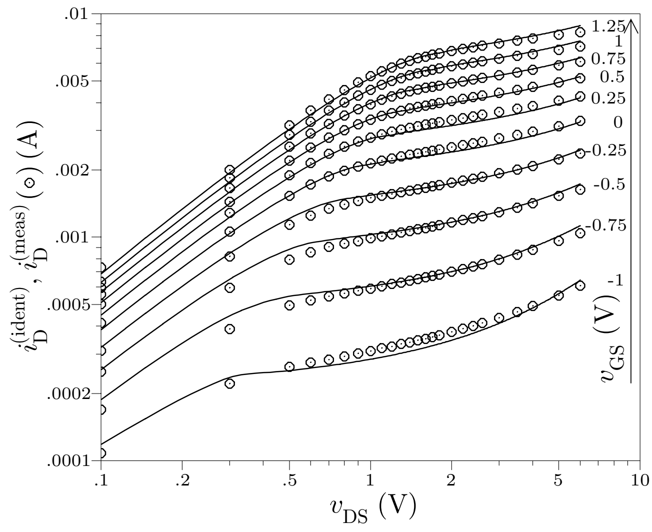

Figure 12: Forward DC characteristics of dep NMOSFET KF521.

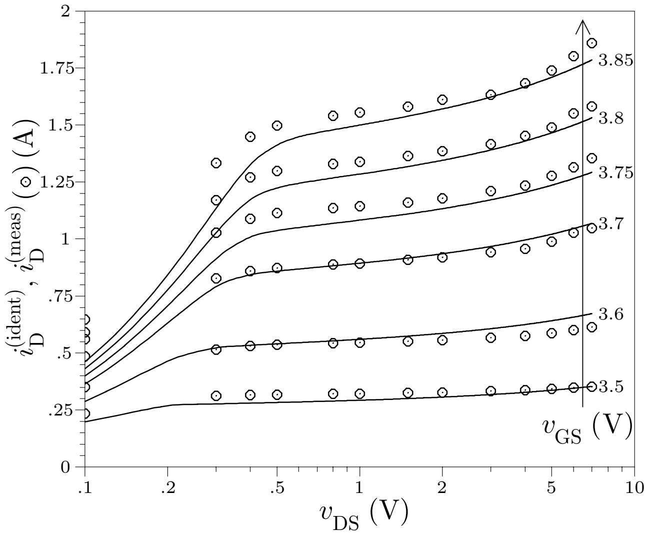

Figure 11: Forward DC characteristics of enh NMOSFET BUZ345.

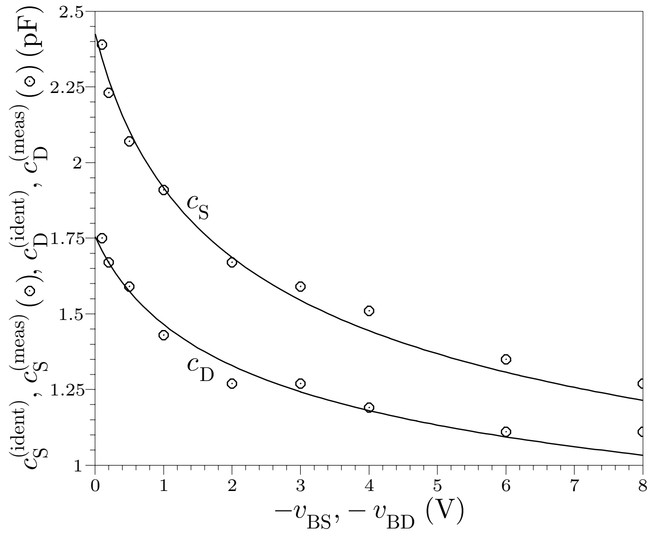

Figure 13: Drain and source junction capacitances of KF521.

2.1 Normalization of the System of Equations

The models of BJT and MOSFET contain values of extreme orders (tiny ones together with the huge ones). For such systems, the standard optimization algorithms are unstable. Therefore, a normalization of differences is included in the C.I.A. program as a new feature (together with their weighting, of course)

$$R_k'\left[\mathbf{x}^{(l)}\right] \triangleq w_k \frac{y_k^{(\mathrm{output})}\left[\mathbf{x}^{(l)}\right] - y_k^{(\mathrm{input})}}{\left|y_k^{(\mathrm{input})}\right| + y_k^{(\mathrm{null})}}, \qquad k = 1, \ldots, m, \quad (6)$$

where (input) and (output) mark measured and optimized values if the optimization is used for the identification purposes. However, many numerical experiments have proved that a normalization of the Jacobian is also necessary:

$$\frac{\partial R_k'\left[\mathbf{x}^{(l)}\right]}{\partial x_i} := w_k \frac{\partial y_k^{(\mathrm{output})}\left[\mathbf{x}^{(l)}\right]}{\partial x_i} \frac{x_i^{(\max)} - x_i^{(\min)}}{\left|y_k^{(\mathrm{input})}\right| + y_k^{(\mathrm{null})}}, \qquad k = 1, \ldots, m,\ i = 1, \ldots, n, \quad (7)$$

where $\partial y_k^{(\mathrm{output})} \big/ \partial x_i$ is a result of *sensitivity* analysis.

The equation (6) is a definition. However, the equation (7) represents an assignment. Therefore, a solution of the system (4) must be modified by the assignment

$$\Delta x_i^{(l)} := \Delta x_i^{(l)} \left[x_i^{(\max)} - x_i^{(\min)}\right],\ i = 1, \ldots, n$$

after each iteration, where $x_i^{(\min)}$ and $x_i^{(\max)}$ represent minimum and maximum allowable values, respectively – they are specified by the user.

The optimization is one of the most important advantages of the C.I.A. program in comparison with the SPICE ones. The total number of optimized circuit parameters is limited to 25. However, there is no problem to increase that number arbitrarily. The optimization may be applied upon the operation point, direct current transfer, frequency, and even transient analyses.

3 The Results of Model Identifications

All the model equations which have been used for the model identifications have been defined in the appendix of The SPICE book [3]. A detailed physical theory on modeling the semiconductor devices is available in [4].

3.1 BJT

3.1.1 A Low Frequency Transistor

The first identified BJT was KC508 which is a Czech equivalent of BC108. The transistor has been firstly identified without the quasisaturation part of the model which is simpler, of course. The results of the identification are shown in Figs. 2 and 3 – the first one (forward mode) with the root mean square (rms) error $9.61\ \%$ and maximum absolute value of relative differences ($\delta_{\max}$) $43.1\ \%$, and the second one (reverse mode) with these values $\mathrm{rms} = 4.85\ \%$ and $\delta_{\max} = 20.0\ \%$.

The optimization has given the values of the model parameters $I_S = 7 \times 10^{-13}$ A, $I_{SE} = 2.98 \times 10^{-11}$ A, $I_{SC} = 1.5 \times 10^{-11}$ A, $\beta_F = 974$, $\beta_R = 50$, $n_F = 1.1$, $n_R = 1.1$, $n_E = 2.06$, $n_C = 1.69$, $V_{AF} = 14.9$ V, $V_{AR} = 4.9$ V, $I_{KF} = 1.2$ A, $I_{KR} = 1.28$ mA, and $r_C = 3.2\ \Omega$.

As shown in Fig. 2, the saturation part of the characteristics is not modeled optimally. Therefore, the equations for modeling the quasisaturation must also be considered. The results of such improved identification are shown in Fig. 4 (they are drawn in natural linear coordinates here in comparison with the two previous logarithmic ones). The optimization has given the additional model parameters $r_{CO} = 10\ \Omega$, $V_O = 100$ V, and $\gamma = 10^{-7}$ [5]. With the inclusion of the quasisaturation, the errors of the identification are lesser than those above – $\mathrm{rms} = 3.51\ \%$ and $\delta_{\max} = 14.9\ \%$.

The parameters of the nonlinear base resistance model are identified using the input characteristic of the transistor as shown in Fig. 5. The input characteristic has been identified with the errors $\mathrm{rms} = 13.5\ \%$ and $\delta_{\max} = 35.0\ \%$ and the optimization has given the model parameters $r_B = 26\ \Omega$, $r_{BM} = 37\ \mathrm{m}\Omega$, $I_{rB} = 3.4$ µA, and $r_E = 0.53\ \Omega$.

The dynamic part of the model has also been identified. Firstly, both junctions capacitances have been determined as shown in Fig. 6. The identification has had the errors $\mathrm{rms} = 1.57\ \%\ (\mathrm{E}),\ 1.64\ \%\ (\mathrm{C})$ and $\delta_{\max} = 2.51\ \%\ (\mathrm{E}),\ 2.73\ \%\ (\mathrm{C})$ and the optimization has given the model parameters $C_{JE} = 4.38$ pF, $\phi_E = 0.65$ V, $m_E = 0.4$, $C_{JC} = 3.11$ pF, $\phi_C = 0.4$ V, and $m_C = 0.273$. Secondly, the transit time model parameters have been identified as shown in Fig. 7. The optimization has given the model parameters $\tau_F = 0.249$ ns, $I_{\tau F} = 0.35$ A, $V_{\tau F} = 8.52$ V, and $X_{\tau F} = 0.33$ with the errors $\mathrm{rms} = 31.8\ \%$ and $\delta_{\max} = 94.4\ \%$. The last ones seem to be large – however, the differences are determined using the "vertical" distances which are not optimal here, of course (actually, the identification can be considered quite successful). The reverse transit time has been identified in the same way with the result $\tau_R = 23$ ns.

3.1.2 A High Frequency Transistor

The second identified BJT was the microwave one: Russian KT391. In Fig. 8, its forward characteristics are shown. The irregularities are probably caused by oscillations during the measurement – it is very difficult to perform the DC measurements for the microwave transistors due to problematic stability of such transistors.

The optimization has given the values of the model parameters $I_S = 10^{-8}$ A, $I_{SE} = 4.7 \times 10^{-9}$ A, $I_{SC} = 10^{-7}$ A, $\beta_F = 133$, $\beta_R = 1.6$, $n_F = 1.15$, $n_R = 1.13$, $n_E = 1.86$, $n_C = 1.75$, $V_{AF} = 123$ V, $V_{AR} = 2$ V, $I_{KF} = 18$ mA, $I_{KR} = 86$ mA, $r_C = 2\ \Omega$, $r_B = 10\ \Omega$, $r_{BM} = 1\ \Omega$, $I_{rB} = 100$ µA, and $r_E = 1.6\ \Omega$ with the identification errors $\mathrm{rms} = 16.0\ \%$ and $\delta_{\max} = 61.7\ \%$. However, if only the triangular "stable" region is used as shown in Figs. 8 and 9, then the errors are lesser: $\mathrm{rms} = 5.99\ \%$ and $\delta_{\max} = 22.2\ \%$ (and the microwave linear transistors are mainly used in such regions...).

3.2 MOSFET

3.2.1 Enhancement Mode Transistors

Firstly, let us identify the models of enhancement transistors. The first one has been the low power standard P-channel 2N3608 – see Fig. 10. The identification procedure has given the values of model parameters $V_{TO} = -4.77$ V, $\phi_S = 0.657$ V, $\phi_O = 0.806$ V, $W = 37.9$ µm, $L = 3.46$ µm, $X_J = 1.54$ µm,

$X_{JL} = 0.762$ µm, $t_{\mathrm{ox}} = 98.7$ nm, $N_{FS} = 10^{15}$ m^{-2}, $N_A = 2.32 \times 10^{22}$ m^{-3}, $v_{\max} = 3.55 \times 10^5$ m/s, $\mu_O = 0.0719$ m^2/(Vs), $E_P = 3.4$ MV/m, $\varkappa = 0.441$, $K_P = 2.49 \times 10^{-5}$ A/V^2, $\gamma = 0.294\ \sqrt{\mathrm{V}}$, $\delta = 0.989$, $\eta = 0.03$, $\theta = 0.00334$ V^{-1}, and $\iota = 0.34$ (the last one is only present in the C.I.A. program where serves as an additional fitting factor). The parameters of the model have been found with a great precision – $\mathrm{rms} = 2.18$ % and $\delta_{\max} = 5.41$ % only!

The second one has been the high power standard N-channel VMOS BUZ345 – see Fig. 11. The identification procedure has given the values of model parameters $V_{TO} = 3.26$ V, $\phi_S = 0.578$ V, $\phi_O = 0.801$ V, $W = 1.46$ m, $L = 4.97$ µm, $X_J = 0.289$ µm, $X_{JL} = 0.179$ µm, $t_{\mathrm{ox}} = 74.7$ nm, $N_{FS} = 10^{15}$ m^{-2}, $N_A = 1.73 \times 10^{20}$ m^{-3}, $v_{\max} = 3.23 \times 10^5$ m/s, $\mu_O = 0.0585$ m^2/(Vs), $\varkappa = 0.0306$, $K_P = 4.19 \times 10^{-5}$ A/V^2, $\gamma = 0.366\ \sqrt{\mathrm{V}}$, $\delta = 1$, $\theta = 0.0384$ V^{-1}, $\iota = 0.572$, $r_D = 0.0249\ \Omega$, and $r_S = 0.0435\ \Omega$ (for the power devices, the drain and source resistances must be identified too; in the previous example, their values have been fixed to the defaults 10 Ω). The identification errors for that power device have been greater than those for the previous one (which is natural): $\mathrm{rms} = 8.67$ % and $\delta_{\max} = 28.8$ %. Moreover, the value of W is extreme but logical – power devices are composed of many single structures and therefore such value represents an integral.

3.2.2 A Depletion Mode Transistor

Secondly, let us identify the model of a depletion-mode transistor which was an N-channel KF521 – see Fig. 12. The identification procedure has given the values of the model parameters $V_{TO} = -1.48$ V, $\phi_S = 0.334$ V, $\phi_O = 0.789$ V, $W = 443$ µm, $L = 4.83$ µm, $X_J = 0.932$ µm, $X_{JL} = 0.827$ µm, $t_{\mathrm{ox}} = 71.8$ nm, $N_{FS} = 10^{15}$ m^{-2}, $N_A = 7.51 \times 10^{21}$ m^{-3}, $v_{\max} = 1.71 \times 10^5$ m/s, $\mu_O = 0.0535$ m^2/(Vs), $E_P = 419$ kV/m, $\varkappa = 0.4$, $K_P = 2.12 \times 10^{-5}$ A/V^2, $\gamma = 0.568\ \sqrt{\mathrm{V}}$, $\delta = 1$, $\eta = 0.811$, $\theta = 0.002$ V^{-1}, $\iota = 0.929$, $r_D = 11.8\ \Omega$, and $r_S = 5.17\ \Omega$. Again, the identification has finished with small errors $\mathrm{rms} = 4.06$ % and $\delta_{\max} = 14.5$ %.

For the KF521 MOSFET, its junction capacitances have also been identified – see Fig. 13. The identification procedure has given the model parameters $C_{JO}\ \mathrm{area}_S = 2.17$ pF, $C_{JO}\ \mathrm{area}_D = 1.57$ pF, $C_{JO\mathrm{sw}}\ \mathrm{perimeter}_S = 0.26$ pF, $C_{JO\mathrm{sw}}\ \mathrm{perimeter}_D = 0.182$ pF, $\phi_O = 0.789$ V, $\phi_{O\mathrm{sw}} = 0.789$ V, $m_S = 0.302$, $m_{S\mathrm{sw}} = 0.183$, $m_D = 0.213$, $m_{D\mathrm{sw}} = 0.286$ – again, the relative errors of the identification are relatively small: $\mathrm{rms} = 2.73$ % (S), 3.15 % (D), $\delta_{\max} = 4.36$ % (S), 6.90 % (D).

4 Conclusion

An optimization algorithm has been presented which is convenient for the robust and effective identifications of complicated tasks. The algorithm has been improved using the equations normalization, which is important for stability of optimizations with BJT and MOSFET. The modified algorithm has been implemented to the C.I.A. program, and typical measurements and identifications of model parameters have been demonstrated.

5 Appendix

The root mean square and maximum deviations computed for the results in Figs. 2–13 are defined naturally

$$\mathrm{rms} = \sqrt{\frac{\sum_{i=1}^{n_p} \left(\frac{y_i^{(\mathrm{ident})} - y_i^{(\mathrm{meas})}}{y_i^{(\mathrm{meas})}} \right)^2}{n_p}} \times 100\,\%,$$

$$\delta_{\max} = \max_{i=1}^{n_p} \left| \frac{y_i^{(\mathrm{ident})} - y_i^{(\mathrm{meas})}}{y_i^{(\mathrm{meas})}} \right| \times 100\,\%,$$

respectively, where $y_i^{(\mathrm{ident})}$ and $y_i^{(\mathrm{meas})}$ are the identified and measured values, and n_p is the number of all the measured points.

Acknowledgement This paper has been supported by the grant of the European Commission TARGET (Top Amplifier Research Groups in a European Team), by the Grant Agency of the Czech Republic, grant No. 102/05/0277, and by the Czech Technical University Research Project MSM 6840770014.

References

[1] Fletcher R. *Practical Methods of Optimization*. John Wiley & Sons, 1978.

[2] Finschi L. An implementation of the Levenberg-Marquardt algorithm. *Eidgenőssische Technische Hochschule Zűrich*, 1996.

[3] Vladimirescu A. *The SPICE Book*. John Wiley & Sons, 1994.

[4] Massobrio G. and Antognetti P. *Semiconductor Devices Modeling With SPICE*. McGraw-Hill, 1993.

[5] Hruškovič L. Quasisaturation Model of BJT. Master's thesis, Czech Technical University, 2004.